**Maximizing Information Extraction from the Mars Global Surveyor Thermal Emission Spectrometer Data.**
A. D. Rogers[1], J. L. Bandfield[2], M. D. Smith[3], and P. R. Christensen[4]. [1]Stony Brook University, Dept. of Geosciences, Stony Brook, NY, USA adrogers@notes.cc.sunysb.edu, [2]University of Washington, Dept. of Earth and Space Sciences, Seattle, WA, USA [3]Goddard Space Flight Center, Greenbelt, MD, USA [4]Arizona State University, School of Earth and Space Exploration, Tempe, AZ, USA.

**Introduction:** A variety of techniques have been used to separate atmospheric and surface contributions in TES spectral data. The most widely used surface-atmosphere separation (SAS) method utilizes a linear least squares fitting routine to model TES emissivity spectra with atmospheric and surface spectra [1]. Atmospheric components (aerosols and gases) are then scaled by their modeled coefficients and subtracted to produce surface-only emissivity. The aerosol end-member spectra were originally derived by *Bandfield et al.* [2], between ~233 and 1301 $cm^{-1}$, excluding the ~508-825 $cm^{-1}$ region. This spectral range was chosen to avoid 1) the strong $CO_2$ fundamental absorption and bracketing $CO_2$ "hot" band absorptions between ~508 and 825 $cm^{-1}$, and 2) $CO_2$ and water vapor isotope absorptions at wavenumbers higher than ~1301 $cm^{-1}$. This results in a maximum of 73 channels that have been used for quantitative surface analysis, out of the full 143-channel range measured by TES in 10 $cm^{-1}$ sampling mode. Some minerals, such as carbonates and dioctahedral smectites, have diagnostic absorptions outside of this spectral range (**Figure 1**).

Since the work of *Bandfield et al.* [2], the correlated-k method [3] has been adopted for removal of $CO_2$ gas absorptions from TES spectral radiance data [4]. The gas removal algorithm of *Bandfield and Smith* [4] also simultaneously corrects for water vapor using the methods of [5]. Gas-corrected TES spectra have been relatively underutilized for compositional studies. The ability to remove the radiative contributions of gas absorptions independently of a linear least squares routine allows us to assess global spectral variability at wavenumbers > 1300 $cm^{-1}$, which includes the carbonate fundamental absorption near ~1550 $cm^{-1}$ as well as diagnostic features arising from volume scattering in dust-covered regions. It also allows us to derive "pure" aerosol end-members as opposed to spectral shapes that encompass both aerosol and gas contributions.

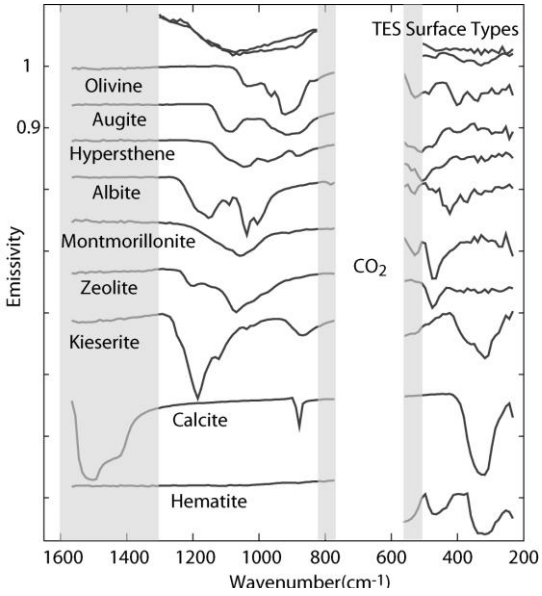


**Figure 1.** Laboratory spectra of select minerals. Shaded areas indicate new spectral range used in this work.

In this work, we improve upon the conventional SAS method by removing gas absorptions and using an extended wavelength range (233-561 $cm^{-1}$ [TES channels 9-40] and 772-1598 $cm^{-1}$ [TES channels 60-138], for a total of 111 channels) for linear least-squares modeling. Here, we derive preliminary aerosol end-members using gas-corrected spectra and apply them to a bright and dark region using the improved SAS methods.

**Methods:** Aerosol end-members were recovered using >2000 daytime radiance spectra selected from multiple orbits that span a range of elevations from the summit to the base of Arsia Mons. The spectra were corrected for gas ($CO_2$ and water vapor) absorptions using correlated-k [e.g., 3] and water vapor index algorithms described above [4-5], and converted to equivalent emissivity. Factor analysis and target transformation techniques [2] were used to determine the number of independently varying components in the data set and recover the spectral shapes of those components. Five independently varying components were identified in the data set, which are: atmospheric dust, water ice, blackbody, slope, and surface dust. Interestingly, *Bandfield et al.* [2] only found 4 components in a similar data set from Arsia Mons; this is most likely due to their exclusion of the short wavelength range (> 1300 $cm^{-1}$), where surface dust has significant spectral features. Using gas-corrected spectra and the newly-derived aerosol end-members from the Arsia Mons data set, we separated the atmospheric and surface contributions in TES spectra for two test regions: a high-albedo surface (TES albedo = 0.29) in Arabia Terra and a low-albedo surface (TES albedo = 0.13) in Mawrth Vallis. The components were separated using a linear least squares minimization routine [e.g. 6].

**Preliminary results: Figure 2** shows the results for the high-albedo surface. The new derived surface emissivity is more similar than the conventionally-derived surface emissivity to "known" dust surfaces from TES multiple emission angle observations [4] and Mini-TES [7].

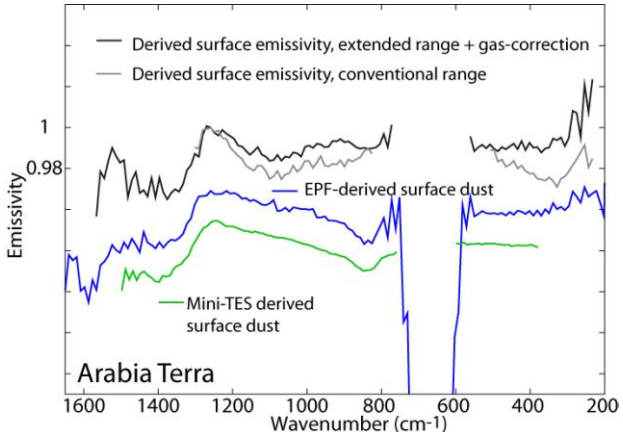


**Figure 2**. Derived surface emissivity from a high-albedo surface in Arabia Terra, compared with average surface dust from TES multiple emission angle observations ("EPF surface dust") [4] and representative surface dust from MER Mini-TES [7]. Using the new SAS parameters results in a significant improvement in derived surface emissivity for this bright region, particularly at low wavenumbers.

**Figure 3** shows surface emissivity spectra from the conventional and new SAS parameters for phyllosilicate-bearing and nearby non-phyllosilicate-bearing surfaces in Mawrth Vallis. Using TES spectral indices designed to map phyllosilicates at 465 and 530 $cm^{-1}$ [8] as well as spectral ratios, [9] concluded that phyllosilicate abundance in this particular area was likely less than 15%, given the lack of a strong 530 $cm^{-1}$ feature [8]. Using the surface emissivity from the extended wavelength range (**Figure 3**), modeled phyllosilicate abundance is less than 5% (areal). We note that this abundance is for the entire area used for the TES spectral average (~200 $km^2$); small-scale exposures of high phyllosilicate abundance are possible. **Figure 3** also illustrates improvement in within-orbit consistency of derived surface emissivity using the new SAS parameters. If atmospheric components are removed consistently between two surfaces of similar temperature and elevation, within the same orbit, then the spectral ratio of the two surfaces should be nearly identical between unatmospherically corrected ("equivalent emissivity") and atmospherically corrected spectra. **Figure 3** illustrates that, using conventional SAS parameters, there is significant deviation in the ratios of derived surface emissivity and equivalent emissivity (blue and green). This indicates inconsistency in the accuracy of SAS in one or both surfaces in the ratio. By contrast, using the new SAS parameters, the surface emissivity ratios are nearly identical to equivalent emissivity ratios, indicating an improvement in consistency.

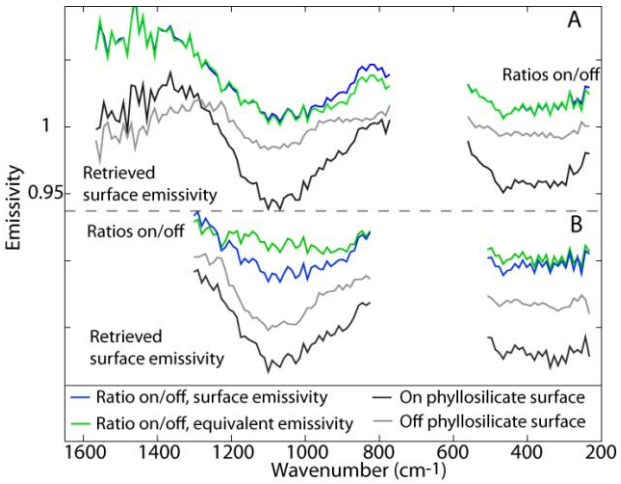


**Figure 3**. Derived surface emissivity spectra from a phyllosilicate-bearing surface and nearby non-phyllosilicate bearing surface in Mawrth Vallis, using **(A)** new and **(B)** conventional SAS parameters. For each case, the ratio of derived surface emissivity spectra is compared with the ratio from unatmospherically-corrected spectra ("equivalent emissivity"). Using new SAS parameters **(A)**, the ratios are nearly identical (compare blue and green), whereas using conventional parameters **(B)**, there is significant deviation between the ratios (compare blue and green). This indicates an improvement in SAS consistency using the new parameters.

**Future work:** Our future work will incorporate small shifts to the spectral sampling of $CO_2$ absorptions at 10 $cm^{-1}$ sampling for the individual TES detectors, which will result in improvements to the gas correction. Global variability in the spectral character at wavenumbers > 1300 $cm^{-1}$ will then be assessed. We will also derive aerosol end-members from a variety of regions and atmospheric conditions, to converge on a set of aerosol end-members that may be applied globally. We will then evaluate the accuracy of the retrieved surface emissivity as well as any systematic changes in surface emissivity/mineral abundance that are evident between the new and conventional SAS methods.

**Acknowledgment:** This work is funded by the NASA Mars Data Analysis Program.

**References:** [1] Smith M. D. et al. 2000, *JGR, 105*, 9589-9607 [2] Bandfield J. L. et al. 2000 *JGR, 105*, 9573-9587 [3] Goody R. et al. 1989 *J. Quant. Spect. Radiat. Transfer, 42*, 539-550 [4] Bandfield J. L. and M. D. Smith 2003, *Icarus, 161*, 47-65 [5] Smith M. D. 2002, *JGR 107*, 5115 doi:10.1029/2001JE001522 [6] Rogers, A. D. and O. Aharonson, 2008, *JGR* E06S14, [7] Glotch T. D. and J. L. Bandfield 2006 *JGR, 111*, E12S06 [8] Ruff S. W. and P. R. Christensen 2007, *GRL 34*, L10204 [9] Rogers A. D. and J. L. Bandfield, 2009 *Icarus, 203*, 10.1016/j.icarus.2009.04.020